Sorption, Desorption, Diffusion, and Permeation of Aliphatic Alkanes into Santoprene Thermoplastic Rubber

TEJRAJ M. AMINABHAVI* and HEMANT T. S. PHAYDE

Department of Chemistry, Karnatak University, Dharwad 580 003, India

SYNOPSIS

The molecular transport characteristics of Santoprene rubber in the presence of *n*-alkanes, cyclohexane, 2,2,4-trimethylpentane, and 1,2,3,4-tetrahydronaphthalene at 25, 40, 55, and 70°C have been studied using a sorption gravimetric technique. From the sorption and desorption studies, the diffusion coefficients have been calculated and used in the discussion of the transport results. It was observed that these data depend on the size of the penetrants. Furthermore, efforts were made to evaluate the permeation coefficients, molar mass between crosslinks, and the kinetic rate constants. These data showed a systematic dependence on the penetrant size. Activation parameters for the process of diffusion and permeation have been calculated from the temperature dependence of the transport coefficients. © 1995 John Wiley & Sons, Inc.

INTRODUCTION

Molecular transport of organic solvents into rubbery polymers is a complex problem with many engineering applications. A detailed description of the diffusion mechanism in such systems depends largely on the ability of the polymer to physically accommodate the permeant molecule, and to continually provide opportunities in the form of randomly generated voids for the aggressive permeant molecule to ingress into the polymer. Many experimental and theoretical investigations in this area have suggested that the size and shape of the permeant molecule and the physical state of the polymer in addition to the usual physical variables such as temperature and solvent concentration are responsible for the study of transport mechanism of small molecules into the rubbery polymer matrices.

Our earlier research activities in this area have been concerned about the molecular transport phenomenon of various organic solvents into a number of engineering elastomers.[1-9] In continuation of this program of research, we now present useful transport data on a thermoplastic "Santoprene"™ rubber membrane (sample designation 201-64) with aliphatic alkanes (C_5–C_{16}), 2,2,4-trimethylpentane, cyclohexane, and 1,2,3,4-tetrahydronaphthalene in the temperature interval 25–70°C. Sorption results for these systems have been analyzed in terms of the Fickian equation to calculate the diffusion coefficients for the Santoprene–alkane systems. Because of the slight departure from the Fickian model, the diffusion parameters have been analyzed in terms of their concentration dependencies. From a temperature dependence of transport coefficients, the Arrhenius activation parameters have been estimated for different transport phenomena.

"Santoprene" is a family of advanced elastomers that successfully combines the performance characteristics of vulcanized rubber such as heat resistance and low compression set with the processing ease of thermoplastics. The blends of ethylene–propylene random copolymer (EPM) and isotactic polypropylene are sold under the trade name of Santoprene. The polymer offers the dual advantages of low-cost thermoplastic processing and vulcanized rubber performance. As a result, it finds rapid acceptance in a variety of industrial and engineering-oriented rubber product applications. The broad spectrum of its performance characteristics makes it exceptionally well-suited for a wider variety of end-use applications such as pump-related gaskets,

* To whom correspondence should be addressed.

Journal of Applied Polymer Science, Vol. 55, 17–37 (1995)
 CCC 0021-8995/95/010017-21

hose connectors, plugs, windshield spacers, body plugs, air ducts, expansion joints, vibration isolators, flexible cords, power-limited circuit cables, submersible cable, filter, and pump seals, etc. However, acceptability of Santoprene for any specific application ultimately depends on its performance and thus, its end-use testing is important before it seeks commercial or engineering applications.

The purpose of the present article is to study Santoprene–alkane interactions as a function of temperature, solvent size, polymer morphology, solvent sorption/desorption, and transport coefficients. In the course of this research, a technique was developed to assess the weight loss of the membrane material to obtain the sorption coefficients. After sorption, polymer samples were desorbed to measure the amount of sorbed solvent and removal of any residual ingredients. The desorbed samples were again exposed to solvent for resorption followed by redesorption. Thus, the sorption (S)–desorption (D)–resorption (RS)–redesorption (RD) testing is an effective method to study the polymer–solvent interactions.

Diffusion, permeation, and equilibrium sorption/desorption coefficients have been determined for Santoprene with the above-mentioned alkanes at 25, 40, 55, and 70°C. The sorption results were analyzed by using the first-order and second-order kinetics relations. Penetration velocities have also been estimated for these systems. Concentration dependencies of diffusion and molar mass between network crosslinks have been calculated to achieve a comprehensive understanding about the nature of the polymer–solvent interactions.

EXPERIMENTAL

Reagents and Materials

Sheets of Santoprene rubber (sample designation 201-64) were procured from Advanced Elastomer Systems, St. Louis, MO (courtesy of Mr. Brant Fletcher) in dimensions of 26 × 26 cm with the initial thicknesses ranging from 0.164 to 0.174 cm. Circular disc-shaped Santoprene samples (diameter = 1.94 to 1.97 cm) were cut from these sheets by means of a sharp-edged carbon-tipped steel die. Because of the slightly hygroscopic nature of the Santoprene rubber, the samples were dried perfectly in a vacuum desiccator over anhydrous calcium chloride at room temperature for at least 24 h before experimentation. Some typical physical and mechanical property data of the samples are given in Table I.

The reagent-grade solvents used as penetrants are: *n*-pentane (BDH, England), *n*-hexane and *n*-heptane (both S.D. Fine Chem. Ltd., Bombay, India), *n*-octane (Riedel, Germany), *n*-nonane, *n*-decane, *n*-dodecane, *n*-tetradecane, and *n*-hexadecane (all from S.D. Fine Chem. Ltd.), 2,2,4-trimethylpentane (BDH, England), cyclohexane (Ranbaxy Labs. Ltd., Punjab, India), and 1,2,3,4-tetrahydronaphthalene (Riedel, Germany). Of these, 2,2,4-trimethylpentane, *n*-dodecane, and 1,2,3,4-tetrahydronaphthalene were double-distilled before use, while other solvents were used as supplied. Their measured physical properties such as density and refractive index at 25°C agreed well with the literature values;[10] however, these data are not given, but only the relevant data of the solvents are summarized in Table II.

Table I Some Typical Mechanical Properties and Fluid Resistance Behavior of Santoprene

Mechanical				Fluid Resistivity[a]		
Properties	ASTM Test Method	Test Temp (°C)	Value	Fluid	Test Temp (°C)	Volume Swelling (%)
Hardness (5 s Shore)	D2240	25	−64A	Water	100	6
Specific gravity	D297	25	0.97	15% NaCl	23	0
Tensile strength (MPa)	D412	25	6.90	50% NaOH	23	0
Ultimate elongation (%)	D412	25	400	98% H_2SO_4	23	5
100% Modulus (MPa)	D412	25	2.3	ASTM #1 Oil	100	31
Tear strength (kN/m)	D624	25	24.5	ASTM #2 Oil	100	50
		100	10.2	ASTM #3 Oil	100	71
Tension set (%)	D412	25	10	Brake fluid	100	−30
Compression set (%)	D395	25	23	Automatic transmission	125	62
168 h		100	36	fluid		
Brittle point (°)	D746	—	−60			

[a] Tested for 166 h.

Table II Some Physical Properties (Viscosity, η, Dielectric Constant, ε, Molar Volume, V, Rao's Molar Sound Function, R, Solubility Parameter, δ, and Molar Refractivity, $[R]$) of Solvents Used as Penetrants at 25°C

Alkane	η (mPa·s)	ε	V (cm^3/mol)	$10^3 \cdot R$ ($[m/s]^{1/3}$ m^3/mol)	δ_S $(cal/cm^3)^{1/2}$	$[R]$ (cm^3/mol)
n-Pentane	0.23[a]	1.84[a]	115	[b]	7.1	25
n-Hexane	0.29	1.88	132	1.35	7.3	30
n-Heptane	0.40	1.93	148	1.54	7.4	35
n-Octane	0.52	1.95	164	1.72	7.6	39
n-Nonane	0.67	1.97	180	1.91	7.7	44
n-Decane	0.86	1.99	196	2.09	7.7	49
n-Dodecane	1.38	2.00	229	2.48	7.8	58
n-Tetradecane	2.04	2.04	260	2.85	8.0	67
n-Hexadecane	3.01	2.09	293	3.22	8.0	76
2,2,4-Trimethyl pentane	0.47	1.94	166	1.70	6.9	[b]
Cyclohexane	0.90	2.02[a]	109	[b]	8.2	[b]
1,2,3,4-Tetra-hydroanaphthalene	2.00	2.77	137	1.55	9.5	[b]

[a] At 20°C.
[b] Values are not calculated.

Sorption (S)–Desorption (D)–Resorption (RS)–Redesorption (RD) Experiments

The circularly cut and perfectly dried polymer samples weighing initially (W_0) $\approx$ 0.4980 g were placed in screw-tight test bottles containing 15–20 mL of the respective solvents. These were periodically removed, the surface-adhered liquid drops were removed by carefully pressing the samples between filter paper wraps, and samples were weighed (W_t) on a digital Mettler balance, Model AE 240 (Switzerland) within the precision of ±0.01 mg. Samples reached equilibrium saturation within 24 h which not changing significantly over a further period of 1 or 2 days. The percent weight gain (wt %) during solvent sorption was calculated as:

$$\text{wt \% } (t) = \left(\frac{W_t - W_0}{W_0}\right) \times 100 \qquad (1)$$

After sorption experiments, the sorbed samples were placed in a vacuum for desorption measurements. The decrease in weight was monitored periodically as before. The total weight loss after desorption was calculated as:

$$\text{wt loss \%} = \left(\frac{W_0 - W_d}{W_0}\right) \times 100 \qquad (2)$$

where W_d is the mass of the polymer after desorption.

The resorption testing was carried out in the same manner as the sorption tests. If the polymer does not show a weight loss during sorption and desorption, the initial weight of the polymer and weight after desorption will be the same. However, in the present research, the weight loss of Santoprene occurred consistently in sorption and resorption experiments for all the solvents. If after a sorption and desorption cycle, the polymer has released all species contributing to the weight loss, the desorption equilibrium solvent content and resorption equilibrium solvent content should be the same. The resorbed samples were placed once again in vacuum for a second desorption. Any difference between the weight loss after redesorption indicates the continued weight loss during resorption. This comparison is another way of testing the extent of the continuous loss during S–D–RS–RD testing. The results confirm the comparison of equilibrium sorption value, M_∞, during desorption and redesorption. The observed total losses in S–D–RS–RD experiments are listed in Table III. The mol % weight change in resorption experiments are generally higher than those observed in sorption experiments indicating higher sorption. However, in desorption and redesorption experiments, the mol % weight change remains almost identical.

RESULTS AND DISCUSSION

Sorption Behavior

Dynamic penetrant transport into the network Santoprene rubber membrane is important because a comprehensive understanding about the mecha-

Table III Mole Percent Weight Change and Total Weight Loss During S–D–RS–RD Cycles at 25°C

Alkane	Mol % Wt Change				Total % Weight Loss After	
	S	D	RS	RD	S–D Cycle	RS–RD Cycle
n-Pentane	0.345	0.731	1.461	[a]	40.3	—
n-Hexane	0.446	0.663	1.445	0.652	40.6	1.86
n-Heptane	0.431	0.584	1.218	0.562	40.4	3.14
n-Octane	0.494	0.539	0.910	0.542	39.1	5.04
n-Nonane	0.379	0.468	1.082	0.459	40.6	2.03
n-Decane	0.350	0.426	1.054	0.425	41.0	1.33
n-Dodecane	0.278	[b]	[b]	[b]	38.8	—
n-Tetradecane	0.229	[b]	[b]	[b]	33.6	—
n-Hexadecane	0.218	[b]	[b]	[b]	[c]	—
2,2,4-Trimethylpentane	0.298	0.489	1.051	0.490	40.5	2.98
Cyclohexane	1.125	0.824	2.735	0.840	40.5	3.20
1,2,3,4-Tetrahydronaphthalene	0.655	0.523	1.519	0.488	40.5	[c]

[a] Experiments not conducted.
[b] Experiments not conducted due to their high boiling points.
[c] Reliable data are not obtained due to incomplete drying.
Abbreviations: S, sorption; D, desorption; RS, resorption; RD, redesorption.

nisms of solvent transport can be achieved. Previous research efforts from our laboratory addressed the mechanisms of solvent transport into a variety of rubbery polymer membranes.[11–14] Continuing these approaches, the dynamic penetrant sorption results have been analyzed in terms of the empirical equation of the type[15]

$$\ln\left[\frac{M_t}{M_\infty}\right] = \ln K + n \ln t \qquad (3)$$

where M_t is solvent uptake at time t, M_∞ refers to solvent sorption at long time, i.e., equilibrium saturation and K is a system parameter which depends on the structural characteristics of the membrane material and on the penetrant/polymer interactions. The exponent value of n indicates the type of transport mechanism and infers any state changes in the macromolecular network. The same pattern of Fickian or non-Fickian behavior was also observed in desorption experiments. In desorption studies, M_t and M_∞ represent, respectively, the mass loss of the drying samples at time t and the completely dried samples. Equation (3) is applicable for a preliminary analysis of sorption data, although at best, it may be useful only up to 55% of the final weight of the solvent sorbed and it has no provisions for analysis of such details as inflection or solvent loss with time. The estimated values of n and K for the sorption and resorption processes are compiled in Table IV. The values of n are accurate to ±0.01 units.

In the majority of cases, the values of n for sorption experiments vary between 0.52 to 0.68 in the investigated temperature range; this suggests that the observed diffusion mechanism is neither Fickian nor non-Fickian, but follows that of anomalous transport.[6–9] The values of n show an increase with temperature. For the resorption process at 25°C, the values of n range from 0.60 to 0.68. The values of the parameter K also increase with a rise in temperature and these depend on the size of the penetrant molecule. The K values decrease systematically with an increase in the molecular size of the penetrants from *n*-pentane to *n*-hexadecane (except *n*-heptane at 25°C) suggesting decreased polymer–solvent interactions. The values of K for cyclohexane are almost identical to that observed for 1,2,3,4-tetrahydronaphthalene and that of 2,2,4-trimethylpentane which at 25°C is the same as that of *n*-octane, but at higher temperatures, *n*-octane exhibits higher K than 2,2,4-trimethylpentane.

A plot of K versus molecular volume of the penetrants in the investigated temperature range is shown in Figure 1. For the resorption process, in all cases, the values of K are about 2 to 3 times smaller than those observed for the sorption process, indicating somewhat milder polymer–solvent interactions. This is justifiable because, during resorption, the available free volume of the polymer is already

Table IV Fitting Parameters of Eq. (3) for Santoprene + Alkanes

	n		10 K, g/g min^n	
	S	RS	S	RS
Alkane	25–70°C	25°C	25–70°C	25°C
n-Pentane	0.67	(0.63)	1.94	(0.78)
n-Hexane	0.59–0.65[b]	(0.61)	1.29–1.91	(0.69)
n-Heptane	0.58–0.68	(0.68)	1.40–1.74	(0.45)
n-Octane	0.58–0.61	(0.63)	1.00–1.54	(0.42)
n-Nonane	0.57–0.60	(0.65)	0.96–1.59	(0.35)
n-Decane	0.58–0.60	(0.62)	0.86–1.38	(0.38)
n-Dodecane	0.57–0.59	[a]	0.69–1.12	[a]
n-Tetradecane	0.56–0.65	[a]	0.50–0.97	[a]
n-Hexadecane	0.54–0.57	[a]	0.52–0.79	[a]
2,2,4-Trimethylpentane	0.58–0.61	(0.60)	1.00–1.38	(0.38)
Cyclohexane	0.62–0.65	(0.65)	0.68–0.97	(0.36)
1,2,3,4-Tetrahydronaphthalene	0.52–0.59	(0.60)	0.59–0.96	(0.26)

[a] Experiments not conducted due to their high boiling points.
[b] Range of temperature is 25–55°C.

filled by the solvent molecules. For the sorption process also, the values of K decrease systematically from *n*-pentane to 1,2,3,4-tetrahydronaphthalene (Table IV).

In the present work, the sorption results are displayed graphically using the normalized parameter, $t^{1/2}/h$ to avoid any differences in the thickness of the Santoprene samples. This convenient presentation shows the possible deviations of the penetrant transport from the Fickian behavior. Reduced plots of the S–D–RS–RD experiments for lower *n*-alkanes (i.e., C_5 to C_{10} including 2,2,4-trimethylpentane i.e., C_8 at 25°C) are presented in Figure 2. For all penetrants, initially the sorption curves showed an overshoot effect as indicated by an abrupt and fast initial penetrant uptake by the polymer. The maxima observed are later followed by a gentle decline to attain the true equilibrium saturation value. Such overshoot effects have been attributed to polymer crosslink density and the increased mobility of the polymer chain segments.[15] Solvent diffuses into the Santoprene network before its chains have had the time to relax (i.e., diffusion is faster than relaxation) and the fractional uptake reaches a maximum (i.e., the overshoot value). When the chains finally relax, the solvent is forced out of the network and hence its uptake eventually reaches the true equilibrium value. Another plausible explanation for the observed overshoot effect is due to the presence of a thin layer formed during the polymerization processes which is morphologically different from the bulk of the polymer. Also, because the solvent diffusion coefficient in the polymer matrix is dependent upon the degree of crosslinking, a sudden initial jump in the uptake is expected if the crosslink density of the polymer is significantly lower in a thin outer layer of the sample. Several studies have addressed different aspects of the overshoot phenomenon when polymers absorb.[16–20] However, overshoot was not observed for the desorption, resorption, and redesorption processes as shown in Figure 2.

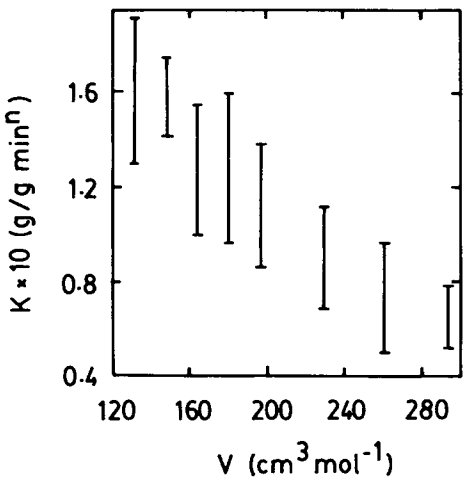

Figure 1 Dependence of parameter K of eq. (3) on molecular volume of *n*-alkanes. Vertical bars indicate the temperature interval of 25–70°C.

The penetrant overshoot effect observed during sorption was analyzed by calculating the percent overshoot index, OI[15] as

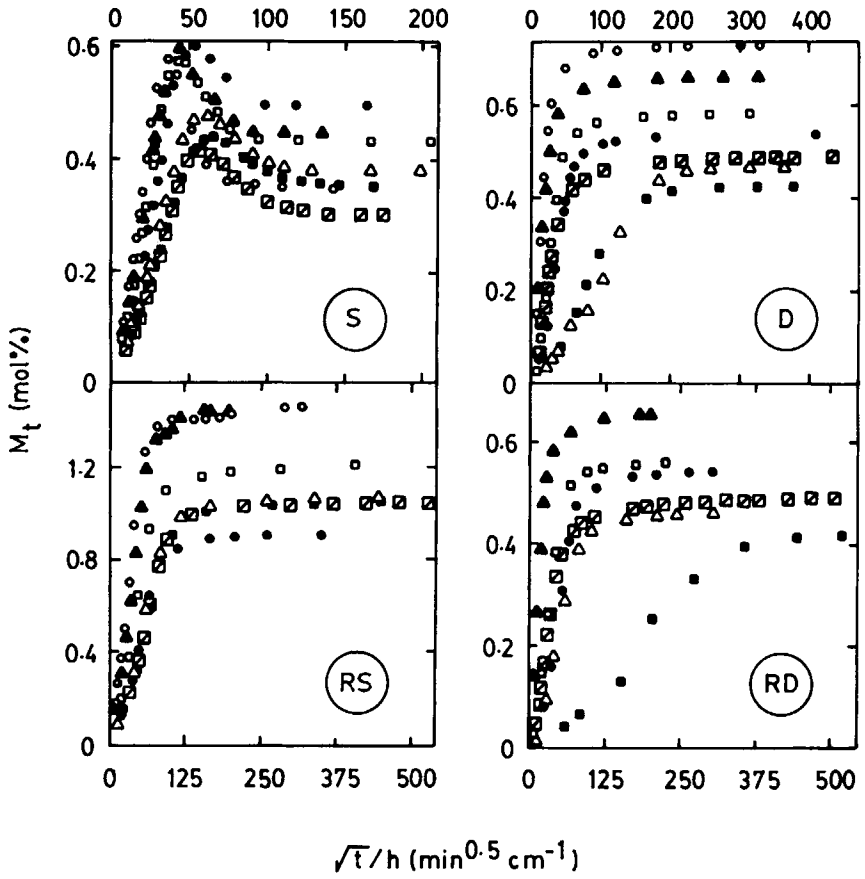

Figure 2 Reduced plots of mol% sorption, desorption, resorption, and redesorption at 25°C for (○) *n*-pentane, (▲) *n*-hexane, (□) *n*-heptane, (●) *n*-octane, (△) *n*-nonane, (■) *n*-decane and (⊠) 2,2,4-trimethylpentane.

$$OI = \frac{M_{max} - M_{\infty}}{M_{\infty}} \times 100 \qquad (4)$$

where M_{max} is the maximum penetrant uptake. The values of *OI* at different temperatures are given in Table V. Generally, the values of *OI* do not show any systematic relationship with either the size of the penetrant molecules or the experimental temperature. Among the penetrants studied, percent overshoot index at 25°C for *n*-pentane is 66.7, which

Table V Percent Overshoot Index Values of Santoprene + Alkanes at Different Temperatures

Alkanes	25°C	40°C	55°C	70°C
n-Pentane	66.7	[a]	[a]	[a]
n-Hexane	33.8	33.5	33.0	[a]
n-Heptane	32.7	33.1	32.6	30.5
n-Octane	21.5	22.5	19.9	18.4
n-Nonane	25.5	23.7	27.1	24.5
n-Decane	25.0	27.4	23.4	21.5
n-Dodecane	25.6	23.4	24.0	22.6
n-Tetradecane	29.3	21.4	20.5	23.0
n-Hexadecane	16.9	18.7	13.8	15.2
2,2,5-Trimethylpentane	38.7	34.9	35.0	30.5
Cyclohexane	8.1	9.6	8.7	7.6
1,2,3,4-Tetrahydronaphthalene	11.0	10.7	8.9	4.6

[a] Data not obtained due to their low boiling points.

is highest among the penetrants considered. The overshoot effect for 2,2,4-trimethylpentane is higher than *n*-octane and also, the *OI* values for 2,2,4-trimethylpentane show a decrease with an increase in temperature. The observed lower value of *OI* of 16.9 for the bigger *n*-hexadecane is attributed to the fact that the relaxational chain rearrangements do not occur as fast as in the presence of a smaller size penetrant such as *n*-pentane. In view of the observed overshoot effect in the present systems, sorption data have also been analyzed by shifting each of the fractional uptake curves from the magnitude of the overshoot effect apparent in the plots (Fig. 2) by using[16]

$$\ln\left[\frac{M_t}{M_\infty}\right] - \ln \alpha = \ln K + n \ln t \qquad (5)$$

where α is a shift factor indicating the initial overshoot effect during sorption. From the least-square estimations of α, K, and n of eq. (5), the values of K and n remain almost identical to those given in Table IV evaluated from eq. (3). In a sorption–desorption cycle, the free volume of the polymer might increase and hence, the sorption process is different from that of the original. These effects are attributed to the relaxation of the polymer network in terms of the times required for the molecular rearrangements of the chains and that of the solvent diffusion into the phantom network polymer. This results in an increase of the polymer segmental mobility due to solvent sorption. This also depends on the ability of solvent molecules to weaken the intermolecular forces of the polymer by disrupting the hydrogen bonds between the chain segments or the efficiency of solvent molecules in increasing the free volume of the polymer.

The resorption curves for *n*-pentane and *n*-hexane are almost identical at 25°C (Fig. 2). Similarly, the resorption curves for *n*-nonane, *n*-decane, 2,2,4-trimethylpentane are almost identical. The resorption values of *n*-heptane are higher than *n*-octane, *n*-nonane, *n*-decane, and 2,2,4-trimethylpentane. The sorption curves of higher *n*-alkanes, viz., *n*-dodecane, *n*-tetradecane, and *n*-hexadecane, and those of cyclohexane and 1,2,3,4-tetrahydronaphthalene are presented in Figure 3. Here again, we observe noticeable overshoot effects especially with *n*-tetradecane and *n*-dodecane, but such effects are less noticeable with penetrants like *n*-hexadecane, cyclohexane, and 1,2,3,4-tetrahydronaphthalene. Also, the equilibrium sorption values are lower for *n*-hexadecane than cyclohexane; 1,2,3,4-tetrahydronaphthalene shows the least value of equilibrium sorption. The desorption curves of some typical penetrants viz., C_5 to C_{10} and 2,2,4-trimethylpentane are presented in Figure 2. It is striking to observe a systematic increase in mol % desorption from C_5 to C_{10}. The desorption curves for *n*-nonane and *n*-decane are slightly sigmoidal suggesting a mild departure from the Fickian mode. The desorption results for higher alkanes, viz., C_{12}, C_{14}, and C_{16} are not obtained due to the difficulties involved in completely drying the polymer samples as these liquids possess high boiling points. The redesorption curves also show identical patterns to those for the desorption process. However, the times required to attain equilibrium desorption are higher in redesorption experiments when compared to desorption results. A striking difference is seen in case of *n*-decane (Fig. 2) which shows a sigmoidal behavior in the redesorption process. It may be noted that the behavior of 2,2,4-trimethylpentane is quite different in S–D–RS–RD experiments (i.e., it exhibits lower sorption or desorption values than its equivalent molecule, *n*-octane).

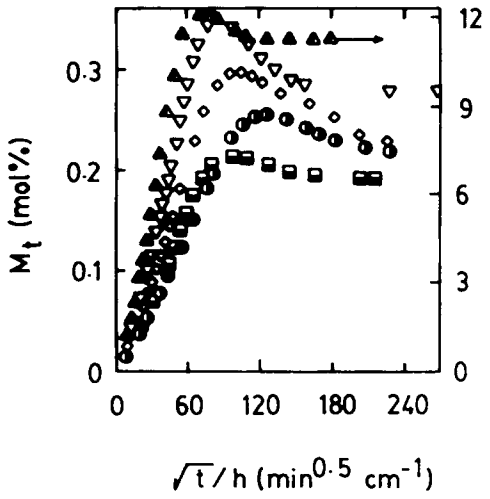

Figure 3 Reduced plots of mol% sorption at 25°C for (▽) *n*-dodecane, (◇) *n*-tetradecane, (◑) *n*-hexadecane, (▲) cyclohexane and (▬) 1,2,3,4-tetrahydronaphthalene.

The sorption results presented in Figure 4 serve as an excellent example of the effect of temperature on the observed sorption behavior of some representative penetrants viz., *n*-heptane, *n*-dodecane, *n*-hexadecane, and 1,2,3,4-tetrahydronaphthalene. It is quite clear that the overshoot effects are persistent even at higher temperatures, but the effect is not very systematic. For 1,2,3,4-tetrahydronaphthalene, the temperature-dependent sorption curves follow a regular pattern (i.e., the sorption values increase with temperature). It may be noted that the final equilibrium values for *n*-heptane and *n*-hexadecane

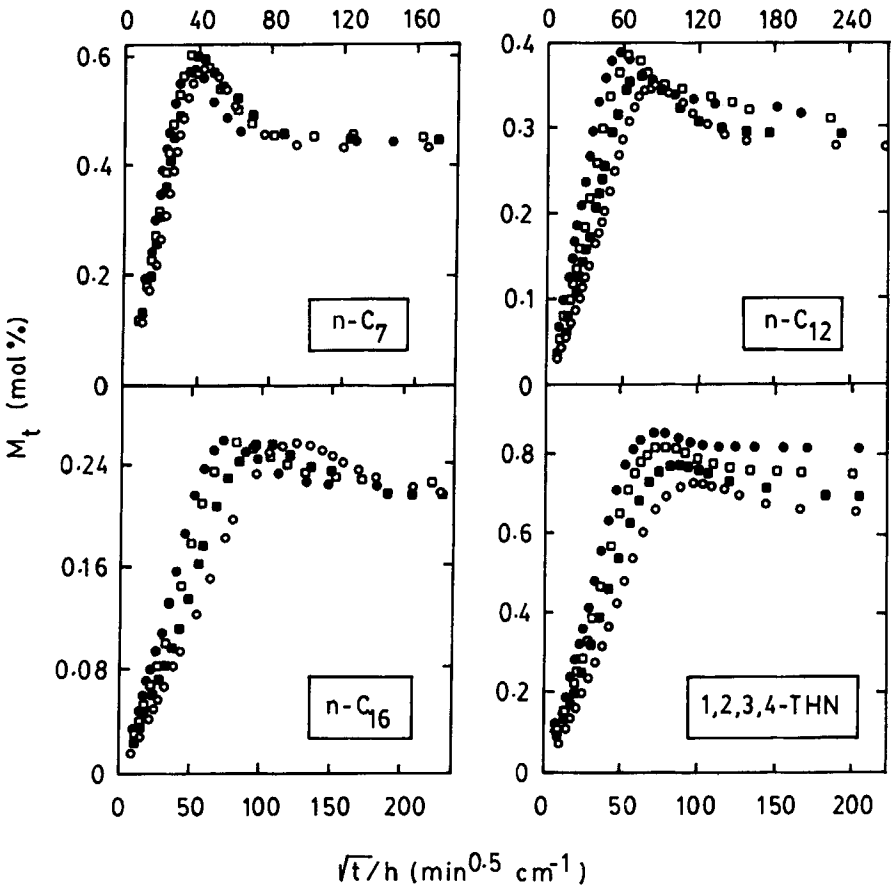

Figure 4 Effect of temperature on sorption curves for *n*-heptane, *n*-dodecane, *n*-hexadecane, and 1,2,3,4-tetrahydronaphthalene. Symbols: (○) 25°C, (■) 40°C, (□) 55°C, (●) 70°C.

lie within a narrow range of equilibrium sorption values. On the other hand, for *n*-dodecane and 1,2,3,4-tetrahydronaphthalene, the final equilibrium values fall within a somewhat wider range. A plausible explanation for this effect is that at high penetrant concentration i.e., during later stages of sorption, the distribution of solvent molecules into the dense region of the polymer network becomes significant. Also, at this stage a significant change in the molecular structure of the polymer might occur.

In desorption, however, a major portion of the total region is lost in the initial period which constitutes only a small fraction of the total experimental time. This probably produces a mismatch of the time scale for diffusion and molecular rearrangement, resulting in a collapsed free volume in the dense region of the polymer which facilitates diffusion and further enhances the effect. However, in the resorption process, large-scale molecular rearrangement does not take place and the diffusion process in these cases may be described as a hole-filling process dominated by the mechanism for the less dense region. Hence, for this process, diffusion coefficient should be constant (see Fig. 2). However, the equilibrium solvent concentration is higher than that observed in sorption experiment (Fig. 2) due to the extra number of pre-existing sufficiently large holes. This phenomenon was also observed by Apicella et al.[21] Since the equilibrium saturation following sorption and resorption is essentially different, the morphology of the polymer is appreciably altered by the S–D–RS–RD experiments.

The mol % sorption coefficients, S obtained from the true equilibrium values of the sorption and resorption processes in the investigated temperature interval are summarized in Table VI. Generally, it is noticed that the mol % sorption values for the sorption processes are considerably smaller than the resorption processes at 25°C. The desorption experiments for *n*-dodecane, *n*-tetradecane, and *n*-hexadecane were not performed due to their high boiling points. The mol % sorption values do not seem to show any systematic dependence on the size of the *n*-alkane penetrants. The values of S for 2,2,4-

Table VI Sorption Coefficients (S) and Penetration Velocities (v) for Santoprene + Alkanes at Different Temperatures Obtained From Sorption and Resorption Experiments

	Temperature, °C				
	25		40	55	70
Alkanes	S	RS		S	
			S, mol %		
n-Pentane	0.345	(1.461)	[a]	[a]	[a]
n-Hexane	0.446	(1.445)	0.448	0.463	[a]
n-Heptane	0.431	(1.218)	0.447	0.452	0.439
n-Octane	0.494	(0.910)	0.511	0.528	0.524
n-Nonane	0.379	(1.082)	0.397	0.409	0.410
n-Decane	0.350	(1.054)	0.344	0.378	0.386
n-Dodecane	0.278	[b]	0.292	0.309	0.316
n-Tetradecane	0.229	[b]	0.247	0.256	0.255
n-Hexadecane	0.218	[b]	0.215	0.225	0.223
2,2,5-Trimethylpentane	0.298	(1.051)	0.321	0.326	0.322
Cyclohexane	1.125	(2.735)	1.187	1.243	1.302
1,2,3,4-Tetrahydronaphthalene	0.655	(1.519)	0.697	0.749	0.816
			10^3 v, cm/s		
n-Pentane	8.603	(2.565)	[a]	[a]	[a]
n-Hexane	5.442	(2.404)	6.719	8.110	[a]
n-Heptane	5.067	(1.975)	6.302	7.754	10.567
n-Octane	3.852	(1.587)	4.665	5.375	6.672
n-Nonane	3.984	(1.406)	5.282	6.328	7.410
n-Decane	3.646	(1.501)	4.628	5.362	6.850
n-Dodecane	2.723	[b]	3.620	4.152	5.472
n-Tetradecane	2.445	[b]	2.830	3.738	5.557
n-Hexadecane	2.028	[b]	2.670	2.942	4.157
2,2,4-Trimethylpentane	3.886	(1.253)	4.514	5.242	6.134
Cyclohexane	1.716	(0.938)	1.903	2.337	2.973
1,2,3,4-Tetrahydronaphthalene	1.643	(0.681)	2.031	2.156	2.690

[a] Data not obtained due to their low boiling point.
[b] Data not obtained due to their high boiling points.

trimethylpentane are significantly smaller than *n*-octane. A longer and bigger molecule such as *n*-hexadecane exhibits an equilibrium sorption of 0.218 mol % as compared to a value of 0.345 mol % for *n*-pentane. Moreover, the value of S for *n*-pentane (0.345 mol %) is almost identical to that of *n*-decane (0.350 mol %). The same dependence is observed for sorption at higher temperatures. It is interesting to note that the equilibrium resorption values at 25°C follow a systematic pattern with the size of the penetrant molecule from *n*-hexane to *n*-hexadecane except *n*-octane. The dependence of maximum and equilibrium sorption values on the size of the *n*-alkanes (i.e., in terms of the number of carbon atoms) is given in Figure 5. From the sorption results given in Table VI, it is obvious that, although 2,2,4-trimethylpentane has 8 carbon atoms, its sorption is not identical to *n*-octane; the sorption of the latter is higher than the former. Also, cyclic penetrants such as cyclohexane and 1,2,3,4-tetrahydronaphthalene exhibit higher values of sorption than all the *n*-alkanes, probably due to their difficulty in migration through the available free volume spaces of the polymer.

The value of equilibrium sorption for *n*-hexane is slightly higher than *n*-heptane at 25°C but, at higher temperatures, viz., 40 and 55°C, sorption of *n*-hexane and *n*-heptane are more or less identical. There is generally not a systematic increase in sorption with an increase in temperature, except in a

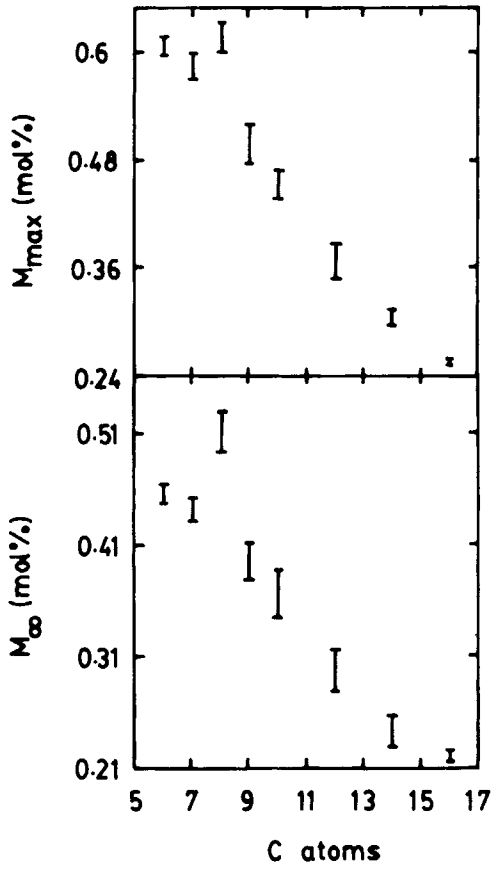

Figure 5 Dependence of maximum (M_{max}) and equilibrium (M_∞) sorption values on the number of carbon atoms of n-alkanes. Vertical bars indicate the temperature interval of 25–70°C.

few cases. The sorption experiments of n-pentane, other than at ambient, and that of n-hexane at 70°C, were not performed due to their low boiling points. Various parameters are critical in the interpretation of sorption results; these include temperature, penetrant size and shape, and polarity in addition to sample history. For instance, an increase in temperature should normally increase sorption; this is due to the creation of extra free volume. Within the investigated temperature range, the dynamic penetrant sorption tends to increase in the temperature interval from 25 to 55°C for all the penetrants except n-heptane and n-octane. However, upon further increasing the sorption temperature up to 70°C, n-heptane and n-octane have shown a decrease in S. This suggests that at 70°C, penetrants like n-heptane and n-octane might interact specifically with the Santoprene chain segments with a possible leaching out of indigenous additives, thereby lowering the equilibrium uptake value. This can be also explained as being due to several reasons: diffusion of residual volatiles, chemical degradation of the groups on the polymer backbone, and diffusion of the residuals due to leaching out of the additives. In the present investigation, the observed effect might be due to the last cause.

Times to attain equilibrium and maximum sorption also play an important role in understanding the transport mechanism. Different equilibrium (T_∞) and maximum (T_m) times are observed depending on the length of the penetrant molecules. Generally, it is observed that the maximum, as well as equilibrium, times increase steadily with an increase in the size of the penetrant molecules (see Fig. 6). It may be noted that the dependence of both T_m and T_∞ values on the chain length of penetrants follow smooth curves.

Penetration Velocity

The penetration velocity, v, of the polymer–solvent pair is related to the moving solvent boundary within the polymer matrix. This was calculated from the weight gain results as[22]

$$v = \frac{1}{2\rho A}\frac{1}{M_\infty}\left(\frac{dW_t}{dt}\right) \tag{6}$$

where dW_t/dt denotes the slope of the weight gain versus time curve and ρ is the density of the polymer; A is the area of one face of the disc shaped polymer sample and factor 2 accounts for penetration from both the surfaces. The area of the circular thickness portion of the disc-shaped sample is also taken into

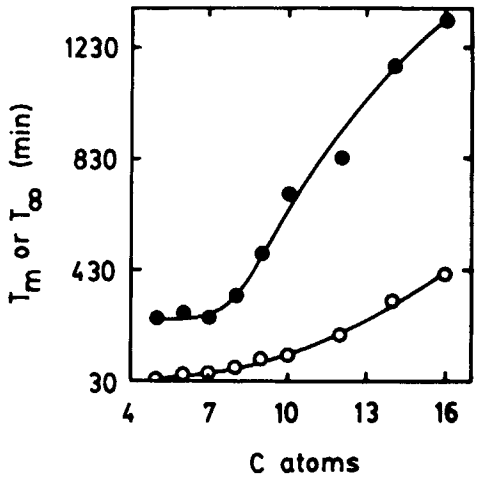

Figure 6 Dependence of maximum (O, T_m) and equilibrium (●, T_∞) times on the number of carbon atoms of n-alkanes at 25°C.

consideration while computing the total area of the sample exposed to the liquid environment. The calculated penetration velocities are also listed in Table VI. Penetration velocities of *n*-alkanes calculated at 25°C follow a systematic decrease from *n*-pentane to *n*-hexadecane (except *n*-octane). The same trend is observed at higher temperatures. The results of v for 2,2,4-trimethylpentane are lower than the equivalent *n*-octane molecule at all the temperatures except at 25°C.

Analysis of Sorption and Desorption Measurements: Calculation of Diffusion Coefficient

Solvent transport into a rubbery polymer is a complex nonsteady-state phenomenon. The diffusion coefficient of the penetrant into such a polymer can be calculated using Fick's second law[23]

$$\frac{\partial C}{\partial t} = \text{div}(D \text{ grad } C) \tag{7}$$

where C is the local concentration of the solvent, t is time, and D is the diffusion coefficient. For a slab geometry of the Santoprene sample immersed in an infinite bath of the liquid, the diffusion coefficient is assumed to be constant. Crank[23] reported different solutions of the Fick's second law depending on the initial and boundary conditions. The case of interest in this article is that of a free film of thickness h, exposed to a uniform and constant concentration of solvent with a zero initial concentration of the diffusant in the film. Thus, the solution to eq. (7) in terms of M_t is given as:

$$M_t = 2M_\infty\left(\frac{Dt}{h^2}\right)^{1/2} \times \left\{\frac{1}{\pi^{1/2}} + 2\sum_{n=0}^{\infty}(-1)^n i \text{ erf } C\left[\frac{nh}{(Dt)^{1/2}}\right]\right\} \tag{8}$$

Equation (8) suggests that a plot of fractional equilibrium uptake versus $t^{1/2}/h$ is linear at small times so that D can be calculated from the initial slope.

At long times, another solution to eq. (7) is preferred for computational purpose which was also used by Allen et al.[24]

$$\frac{M_t}{M_\infty} = 1 - \left(\frac{8}{\pi^2}\right) \times \sum_{n=0}^{\infty}\left\{\left[\frac{1}{(2n+1)^2}\right]\exp\left[\frac{-D(2n+1)^2\pi^2 t}{h^2}\right]\right\} \tag{9}$$

In deriving eq. (9), the diffusion coefficient is assumed to be constant. The calculated diffusion coefficients are given in Table VII. Equation (9) at longer diffusion time can be simplified to give

$$\ln(1 - M_t/M_\infty) = \ln\left(\frac{8}{\pi^2}\right) - \frac{D\pi^2 t}{h^2} \tag{10}$$

Thus, a plot of $\ln(1 - M_t/M_\infty)$ versus t should be linear at long diffusion times and the slope is directly proportional to D. Our data have been plotted in this format, which are in conformity with eq. (10) (see Fig. 7).

The diffusion coefficients obtained by using eq. (10) are somewhat higher than the D values calculated from eq. (9). This is expected because of the consideration of the long-term diffusivity while calculating D from eq. (10). However, we regard the values of D calculated from eq. (9) as more reliable. A systematic decrease in D with an increase in the size of the penetrants from *n*-pentane to *n*-hexadecane (except *n*-heptane at 25°C) is observed at all the temperatures. A plot of D versus number of carbon atoms showing this effect is shown in Figure 8. This type of dependence has been also obtained in the literature.[25–27] A linear and flexible molecule is expected to diffuse faster than a somewhat less flexible and less symmetrical molecule such as 2,2,4-trimethylpentane, cyclohexane, and 1,2,3,4-tetrahydronaphthalene. It was found that at all the temperatures studied, the values of D for 2,2,4-trimethylpentane are lower than the expected values of a linear molecule of the same size such as *n*-octane. This is because the presence of pendant methyl groups in 2,2,4-trimethylpentane render its molecular diameter larger; thus, the molecule may not locate an appropriate hole for its transport in the polymer matrix.

Diffusion of a number of homologous paraffin hydrocarbons has been studied[28] wherein it was observed that the side methyl groups in the penetrants lowered the diffusivities more than in the case of the corresponding linear molecules. Conversely, when penetrant molecules are of comparable diameter but of varying length, the effect of length of the molecule will play a dominant role. This was the case for *n*-hexadecane, whose diffusion coefficients are smaller than other lower *n*-alkanes. The diffusion coefficients of cyclohexane fall between *n*-decane and *n*-dodecane, and those of 1,2,3,4-tetrahydronaphthalene fall between *n*-tetradecane and *n*-hexadecane.

An important feature of the Fickian sorption is that both sorption and desorption curves are linear

Table VII Diffusion (D) and Permeation (P) Coefficients of Santoprene + Alkanes from Sorption Measurements at Different Temperatures

Alkanes	Temperature, °C			
	25	40	55	70
		10^6D, cm^2/s		
n-Pentane	6.07	[a]	[a]	[a]
n-Hexane	2.88	3.83	4.63	[a]
n-Heptane	3.22	3.74	4.72	4.82
n-Octane	1.83	2.36	2.88	3.64
n-Nonane	1.69	2.23	2.87	3.79
n-Decane	1.34	1.78	2.10	2.67
n-Dodecane	0.78	1.04	1.44	2.05
n-Tetradecane	0.62	0.69	1.08	1.49
n-Hexadecane	0.34	0.55	0.74	0.97
2,2,4-Trimethylpentane	1.66	2.07	2.40	3.05
Cyclohexane	0.90	1.27	1.74	1.90
1,2,3,4-Tetrahydronaphthalene	0.56	0.80	0.93	1.19
		10^6P, cm^2/s		
n-Pentane	1.51	[a]	[a]	[a]
n-Hexane	1.11	1.48	1.85	[a]
n-Heptane	1.39	1.67	2.13	2.12
n-Octane	1.03	1.38	1.73	2.18
n-Nonane	0.82	1.13	1.50	1.99
n-Decane	0.67	0.87	1.13	1.47
n-Dodecane	0.37	0.52	0.76	1.10
n-Tetradecane	0.28	0.34	0.55	0.75
n-Hexadecane	0.17	0.27	0.38	0.49
2,2,4-Trimethylpentane	0.56	0.76	0.89	1.12
Cyclohexane	0.85	1.27	1.82	2.08
1,2,3,4-Tetrahydronaphthalene	0.49	0.74	0.92	1.29

[a] Data not obtained due to their low boiling points.

with $t^{1/2}/h$ in the initial stages. In some cases, (e.g., with *n*-pentane or *n*-hexane), the linear sorption region extends up to almost 70% of M_∞. The departure from the Fickian diffusion occurs for many reasons. For example, if sorption equilibrium cannot be achieved at the membrane surface, the sorption curves exhibit an inflection and show a non-Fickian trend (abnormal type). Diffusion of penetrant molecules into polymers depends on two factors viz., the availability of appropriate molecular size holes in the network and the attractive forces between the penetrant molecules and the polymer. The presence of holes is determined mainly by the polymer structure and morphology reflected in its stiffness and ability to closely pack in the amorphous state. The formation of an appropriate hole also depends on the cohesive energy density of the polymer and on the penetrant amount.

Santoprene is a lightly crosslinked polymer having dense regions distributed randomly in the whole of the matrix. When such an elastomer is immersed in a solvent, the solvent diffusion into the polymer expands the system, and thereby weakens the molecular interaction between the neighboring polymer chains. This implies that the polymer chains between crosslinks move more freely, and hence the molecular mobility of the network chains is enhanced through the diffusion of the solvent. However, the fraction of the constrained regions of the network chains may decrease through an interaction between the network chains of the polymer and the solvent molecules. A highly crosslinked polymer structure will inhibit the diffusion process more than a linear polymer because such chains are more tightly bound together and resist the separation necessary to form a void capable of accommodating

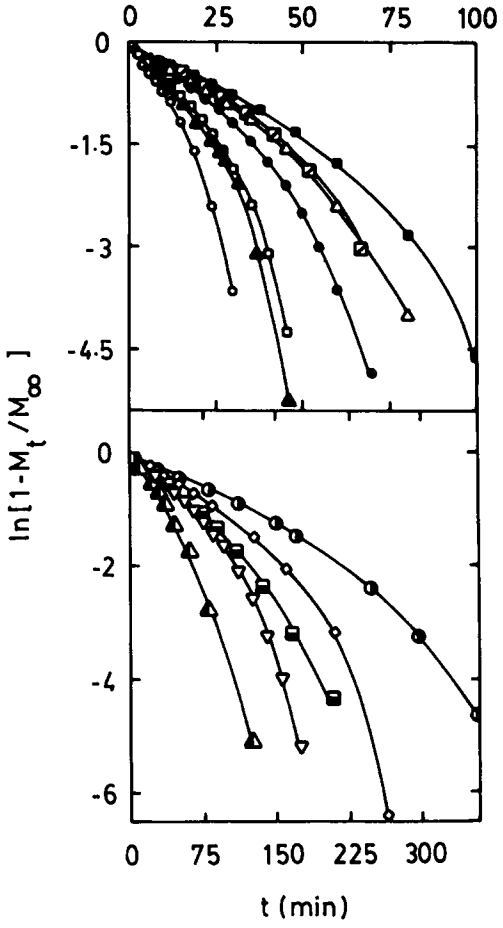

Figure 7 Long-term diffusion plots for Santoprene + n-alkanes at 25°C. Symbols are the same as in Figures 2 and 3.

a diffusing molecule. The energy to create such voids will therefore be large and the permeability is small. Such structural tightness is found not only in highly crosslinked polymers but also in those possessing a high degree of crystallinity, symmetry or strong cohesive forces brought about by the polarity effects. The opposite effect will occur if there are none of these features and the polymer network is loose. This is usually most possible in plasticized materials and those containing double bonds such as in Santoprene.

Diffusion in rubbery polymers also seems to bear a direct relationship with some of the important properties such as viscosity, dielectric constant, refractive index, and speed of sound of solvents. Recently, Vahdat[29] investigated a correlation between diffusivity and viscosity for elastomer–solvent systems. To see such a dependence in the present systems, we found that other liquid state properties like viscosity η, and dielectric constant ε, also show a

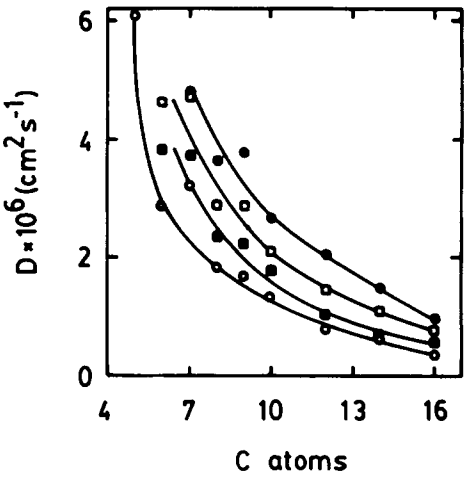

Figure 8 Dependence of diffusion coefficient on the number of carbon atoms of n-alkanes at temperatures given in Figure 4.

systematic dependence on penetrant diffusivity (Fig. 9). Similarly, the molar refraction [R], of the liquid calculated from the Lorenz–Lorentz formula,[30]

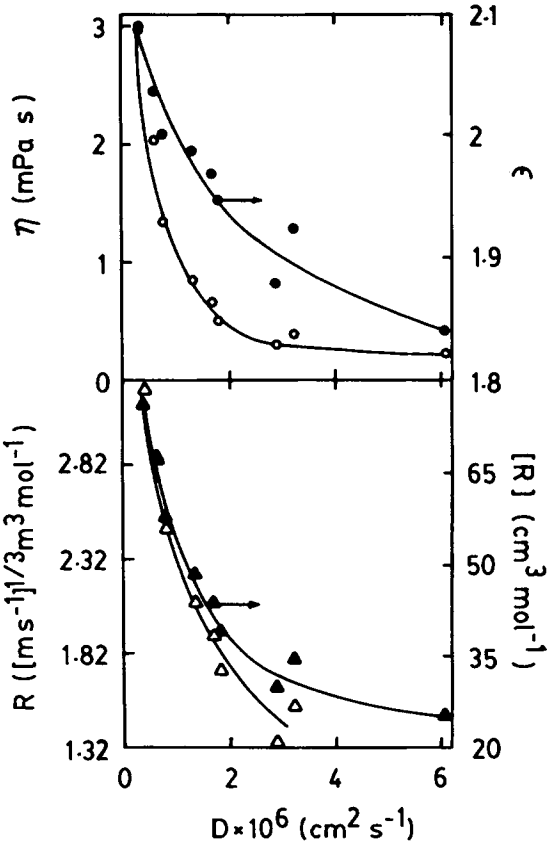

Figure 9 Relationship between (○) viscosity, (●) dielectric constant, (▲) molar refractivity, and (△) Rao's molar sound function with diffusivity for Santoprene + n-alkanes at 25°C.

Table VIII Comparison of Diffusion and Permeation Coefficients from S–D–RS–RD Experiments at 25°C for Santoprene + Alkanes

Alkanes	S	D	RS	RD
		10^6D, cm^2/s		
n-Pentane	6.07	2.35	0.86	[a]
n-Hexane	2.88	2.17	0.65	2.27
n-Heptane	3.22	0.44	0.48	0.28
n-Octane	1.83	0.27	0.31	0.08
n-Nonane	1.69	0.03	0.27	0.11
n-Decane	1.34	0.03	0.24	0.004
2,2,4-Trimethyl pentane	1.66	0.46	0.22	0.35
Cyclohexane	0.90	0.003	0.28	1.22
1,2,3,4-Tetrahydronaphthalene	0.56	0.01	0.11	[b]
		10^6P, cm^2/s		
n-Pentane	1.51	1.24	0.91	[a]
n-Hexane	1.11	1.24	0.80	1.27
n-Heptane	1.39	0.26	0.58	0.16
n-Octane	1.03	0.17	0.32	0.05
n-Nonane	0.82	0.02	0.38	0.06
n-Decane	0.67	0.02	0.37	0.002
2,2,4-Trimethylpentane	0.56	0.26	0.27	0.20
Cyclohexane	0.85	0.80	0.65	0.86
1,2,3,4-Tetrahydronaphthalene	0.49	0.002	0.22	[b]

[a] Experiments are not conducted.
[b] Reliable data are not obtained.

$$[R] = \frac{n^2 - 1}{n^2 + 2}\frac{M}{\rho} \tag{11}$$

(where M is molecular weight of the liquid, ρ is its density and n is the refractive index) also shows a decreasing trend with diffusion coefficients. Also, Rao's molar sound function R, calculated from the speed of sound u, data of the liquids[31]

$$R = u^{1/3}V \tag{12}$$

shows the same dependency (see Fig. 9).

In continuation of our earlier studies,[11–14] the values of the permeability coefficient P, have been calculated as: $P \equiv D \cdot S$, and these data are also included in Table VII. It is generally observed that permeability data follow the same pattern as those of diffusion coefficients in the investigated temperature range. Permeabilities of cyclohexane and *n*-nonane are somewhat identical. Similarly, permeabilities of 1,2,3,4-tetrahydronaphthalene lie between those of *n*-decane and *n*-dodecane. Permeabilities of *n*-octane are higher than those of 2,2,4-trimethylpentane. A comparison of diffusion and permeation coefficients at 25°C for the S–D–RS–RD experiments is made in Table VIII. The values of these coefficients are different in all these processes, suggesting possible morphological changes in Santoprene in the presence of different penetrants during cyclic S–D–RS–RD testing. The values of diffusion and permeation coefficients are considerably smaller in the cases of *n*-nonane and *n*-decane in desorption and redesorption experiments when compared to other penetrants. Similarly, diffusion and permeation coefficients for cyclohexane and 1,2,3,4-tetrahydronaphthalene are extremely small.

Concentration Dependence of Diffusion Coefficients

Several studies have indicated that diffusion in rubbery polymers deviates from the classical Fickian mechanism through a concentration-dependent diffusion. When sorption proceeds with time, the concentration continues to build up at the membrane surface and later, toward its interior. As a result, the diffusion coefficient becomes concentration-dependent. To investigate this effect, attempts have been made to analyze the concentration dependence

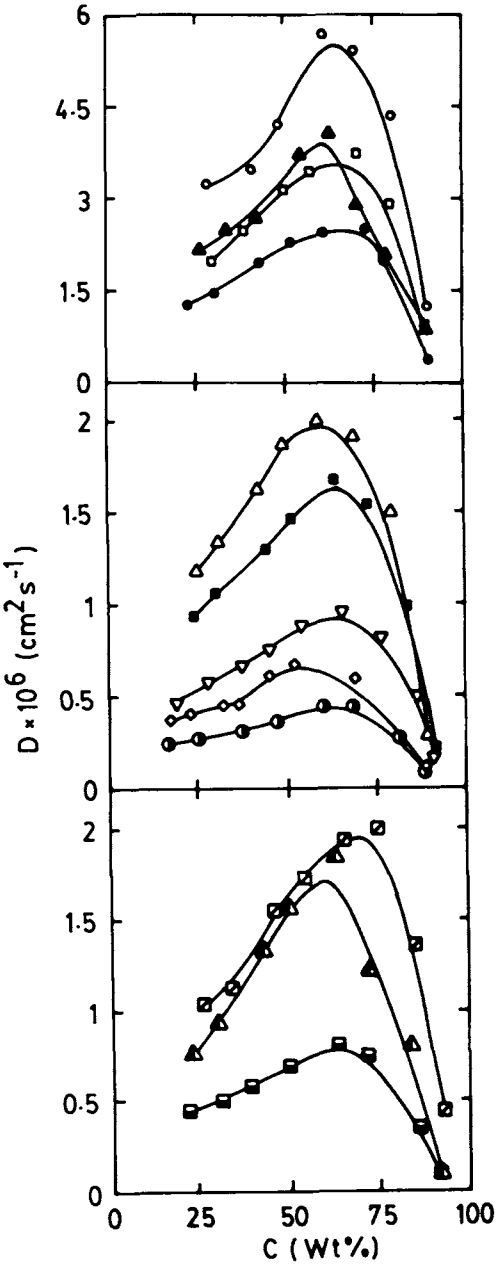

Figure 10 Concentration dependence of diffusion coefficient for Santoprene + alkanes at 25°C. Symbols are the same as in Figures 2 and 3.

of diffusivity for those systems exhibiting anomalous or nearly non-Fickian diffusion behavior.

The computer-generated plots of D versus wt % concentration for n-pentane to n-octane, n-nonane to n-hexadecane, and for 2,2,4-trimethylpentane, cyclohexane, and 1,2,3,4-tetrahydronaphthalene at 25°C are presented in Figure 10. It is found that in majority of cases, we observe a nearly Gaussian type behavior with the maximum being observed around 70 wt % penetrant concentration. The maxima decrease systematically from a smaller to a bigger molecule. These observations are consistent with the swelling tendency of the membrane in the presence of n-alkanes. The observed maxima of diffusion versus concentration are attributed to the competing contributions of the solvent mobility and the thermodynamic equilibrium factor. This observation is consistent with the report of Feng et al.[32] on dichloroethane transport into a phase-segregated polyurethane membrane.

Kinetics of Sorption

Almost all crosslinked polymers exhibit swelling when brought in contact with aggressive solvent media. Such swelling in these polymers is attributed to the phenomenon of sorption kinetics. It has been shown earlier[14] that sorption in rubbery polymers can be treated by using first-order kinetics. Con-

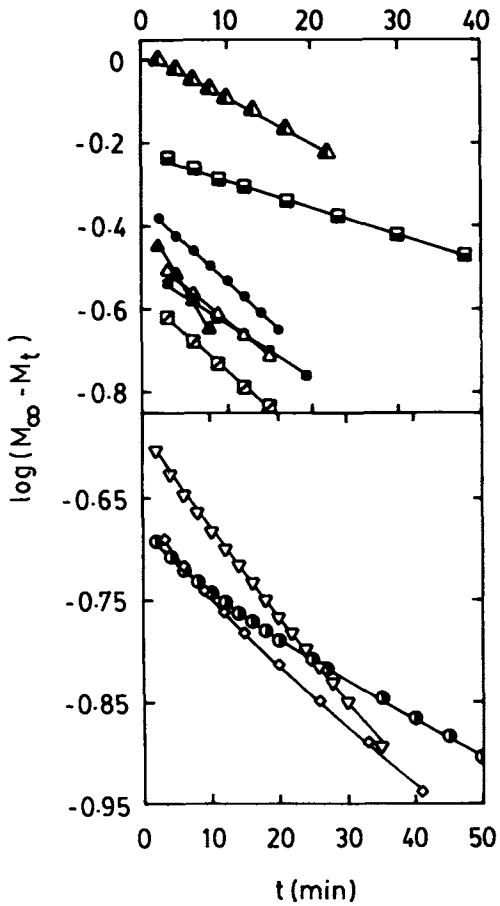

Figure 11 First-order kinetic plots for Santoprene + alkanes at 25°C. Symbols are the same as in Figures 2 and 3.

Table IX First-Order (k_1) and Second-Order (k_2) Rate Constants for Santoprene + Alkanes at Different Temperatures Obtained from Sorption and Resorption Experiments

	Temperature, °C				
	25		40	55	70
Alkanes	S	RS	S		
			10^2k_1, min^{-1}		
n-Pentane	15.48	(3.45)	[a]	[a]	[a]
n-Hexane	7.64	(2.62)	9.48	11.25	[a]
n-Heptane	6.68	(2.01)	7.94	9.96	12.89
n-Octane	4.40	(1.44)	5.28	6.30	7.66
n-Nonane	3.92	(1.17)	5.42	6.59	7.75
n-Decane	3.22	(1.05)	4.22	4.81	6.28
n-Dodecane	1.98	[b]	2.65	3.14	4.26
n-Tetradecane	1.48	[b]	1.78	2.39	3.38
n-Hexadecane	0.98	[b]	1.42	1.61	2.24
2,2,4-Trimethylpentane	4.14	(1.00)	4.79	5.47	6.91
Cyclohexane	2.55	(1.23)	2.98	4.00	4.70
1,2,3,4-Tetrahydronaphthalene	1.52	(0.51)	1.88	2.11	2.63
			$10k_2$, mol^{-1} min^{-1}		
n-Pentane	21.00	(1.65)	[a]	[a]	[a]
n-Hexane	6.45	(1.02)	7.89	9.21	[a]
n-Heptane	5.18	(0.95)	5.66	7.30	9.34
n-Octane	2.61	(0.72)	2.89	3.51	4.27
n-Nonane	2.54	(0.43)	2.84	4.25	4.85
n-Decane	2.04	(0.34)	3.69	2.85	3.90
n-Dodecane	1.35	[b]	1.75	1.90	2.63
n-Tetradecane	0.97	[b]	1.14	1.48	2.02
n-Hexadecane	0.57	[b]	0.94	0.99	1.36
2,2,4-Trimethylpentane	4.03	(0.40)	4.16	4.50	6.29
Cyclohexane	0.82	(0.28)	0.89	1.26	1.38
1,2,3,4-Tetrahydronaphthalene	0.54	(0.13)	0.61	0.65	0.77

[a] Data not obtained due to their low boiling points.
[b] Experiments not conducted due to their high boiling points.

tinuing this approach, the values of the first-order kinetic rate constants k_1 have been calculated as:

$$dM/dt = k_1(M_\infty - M_t) \tag{13}$$

which upon integration gives

$$k_1 t = \ln[M_\infty/(M_\infty - M_t)] \tag{14}$$

A representative plot of $\log(M_\infty - M_t)$ versus t is shown in Figure 11. Different negative slopes are observed for different solvents and this is attributed to different solvent sorptivities. The calculated rate constants from 25 to 70°C are given in Table IX. The kinetic rate constants follow the regular trend of increase with temperature and show a decreasing trend with an increase in the size of the penetrant molecule. This is expected in view of the fact that diffusivity values are directly proportional to the k_1 values as shown in the following treatment.

For long sorption times, the term $n \geq 1$ as well as $\ln(8/\pi^2)$ can be ignored so that eq. (9) simplifies to give

$$\ln\left(\frac{M_\infty}{M_\infty - M_t}\right) \cong \frac{\pi^2 Dt}{h^2} \tag{15}$$

Equation (15) is identical to eq. (14) when

$$k_1 = \frac{\pi^2 D}{h^2} \tag{16}$$

For extensive swelling, h^2 does not remain constant and hence, D increases due to the influx of the solvent molecules into the polymer matrix. As long as the increase in D matches h^2, the values of k_1 in eq. (16) remain nearly constant, so that eq. (14) or eq. (15) is obeyed approximately and first-order kinetics are applicable to these systems. When swelling becomes considerable, and the increase in h^2 exceeds the increase in D to a point where the variation in k_1 and deviation from the first-order kinetics become somewhat significant, then it may be legitimate to apply the second-order kinetics model from the following empirical equation.[33-35]

$$\frac{t}{C} = A + Bt \tag{17}$$

where A and B are numerical constants and C is concentration. At long times, $Bt \gg A$ so that, $B = 1/C_\infty$. At short times, $A > Bt$ so that, the quantity $\frac{1}{A} = \lim_{t\to 0}\left(\frac{dC}{dt}\right)$ represents the initial rate of swelling, when the polymer network just begins to relax in response to the osmotic pressure. The equation for second-order swelling is then given as

$$\frac{dC}{dt} = k_2(M_\infty - M_t)^2 \tag{18}$$

where k_2 is the second-order rate constant. The integrated form of the equation representing swelling rate at time, t is given by

$$M_t = \frac{k_2 M_\infty^2 t}{1 + k_2 M_\infty t} \tag{19}$$

which upon further simplification gives

$$k_2 t = \frac{M_t}{M_\infty(M_\infty - M_t)} \quad \text{or}$$

$$k_2 t = \frac{1}{M_\infty - M_t} - \frac{1}{M_\infty} \tag{20}$$

where $k_2 = 1/AC_\infty^2$. The dimensions of k_2 are concentration^{-1} and time^{-1} (see Table IX). A detailed explanation for the use of the second-order swelling kinetics has been given by Schott.[33]

A typical second-order kinetic plot for alkanes at 25°C (Fig. 12) supports the use of the second-order kinetic equations to analyze the data of this study. The second-order kinetics plot follows the curvature behavior over the extended region of swelling. However, in order to estimate the second-order kinetic rate constants, we need to consider only the initial portion of the swelling curve. The early portion of this curve is a straight line and from the slope of this curve, the values of k_2 were calculated. These values are smaller than the k_1 values for all the Santoprene + solvent systems and show almost the same dependence on the penetrant size and temperature as those of the k_1 values discussed above.

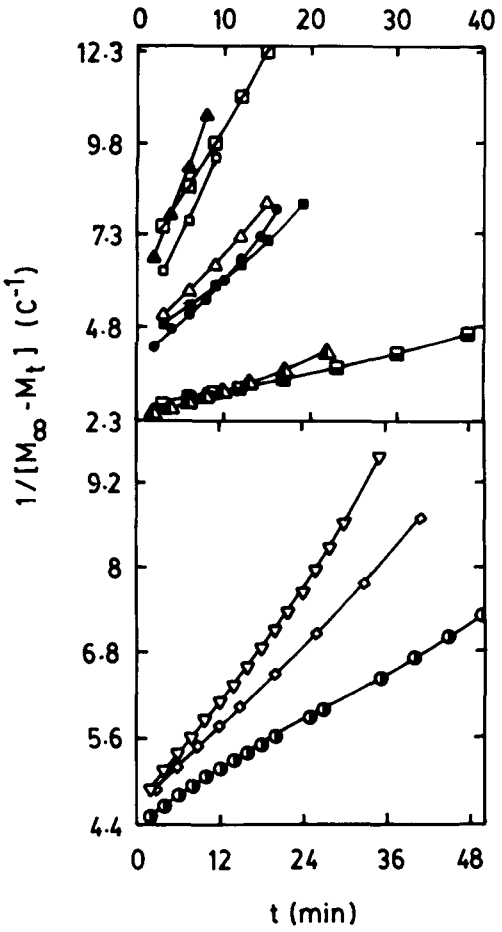

Figure 12 Second-order kinetic plots for Santoprene + alkanes at 25°C. Symbols are the same as in Figures 2 and 3.

Effect of Temperature and Activation Parameters

Advances have been made over the past several years to develop a microscopic description of the diffusion phenomenon in polymers; diffusion in rubbery polymers is quite different from that in glassy polymers.[36] According to the molecular models of rubbery polymers above their glass transition temperatures, the Arrhenius relation is generally valid experimentally, but curved plots are observed in cases when larger temperature ranges are used.[37] The present experi-

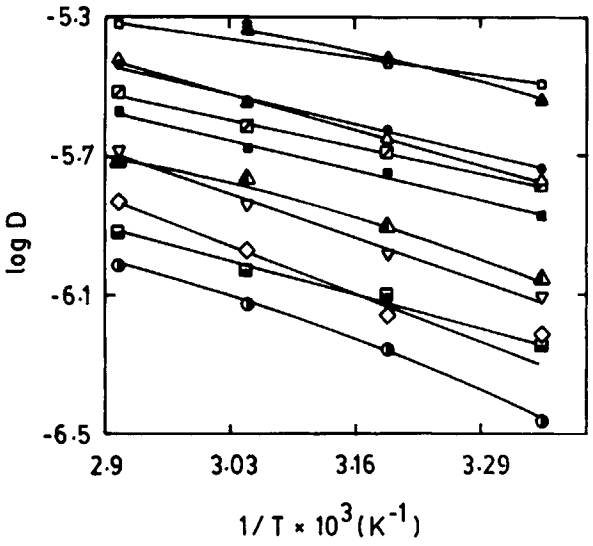

Figure 13 Arrhenius plots for the dependence of log D vs. $1/T$ for Santoprene + alkanes. Symbols are the same as in Figures 2 and 3.

mental results have been analyzed using the Arrhenius relation for the diffusion process as

$$D = D_0\exp(-E_D/RT) \tag{21}$$

where E_D is the activation energy of diffusion which is a function of the intra- and interchain forces that must be overcome in order to create the space for a unit diffusional jump of the penetrant molecule; D_0 is a pre-exponential factor and RT has the conventional meaning. The activation energy will be greater the larger the penetrant molecule, the stronger the polymer cohesive energy, and the more rigid the polymer chain segments.

In an analogous manner, the sorption coefficient S, can be expressed in terms of the van't Hoff relationship with a pre-exponential factor S_0, as:

$$S = S_0\exp(-\Delta H_S/RT) \tag{22}$$

where ΔH_S is the heat of sorption and is a composite parameter involving the contributions from: (1) Henry's law, needed for the formation of a site and the dissolution of the species into that site; the formation of a site usually involves an endothermic contribution and (2) Langmuir's (hole filling) type sorption mechanisms, in which case the site already exists in the polymer matrix and sorption by the hole-filling mechanism gives exothermic heats of sorption.

Because the transport phenomenon involves both the sorption and diffusion processes, the permeability coefficient, may also be expressed similarly so that the activation energy, E_P for the process of permeation is:

$$E_P = E_D + \Delta H_S \tag{23}$$

Since in the present systems the values of S, P, and D have shown an increase with a rise in temperature, eqs. (21) and (22) were used to calculate E_D and ΔH_S values from the least-squares procedure. Figure 13 displays the plots of log D versus $1/T$ wherein the dependence follows almost linearly in the investigated range of temperature. Using eq. (23), the E_P values were calculated. These results are summarized in Table X. It is noticed that, unexpectedly, the results of E_D or E_P do not show any regular trend with the size of the penetrant. The lowest value of E_D and E_P of about 8 kJ/mol is observed for n-heptane, while the highest value of E_D, of about 20 kJ/mol, is found for n-hexadecane. Activation param-

Table X Activation Parameters (E_D, E_P, and ΔH_S All in kJ/mol), Interaction Parameter (χ) and Molar Mass Between Crosslinks ($\bar{M}_C$) for Santoprene + Alkanes

Alkanes	E_D	E_P	ΔH_S	χ	$\bar{M}_C$
n-Hexane	12.87	13.86	0.99	0.360	302
n-Heptane	8.23	8.64	0.41	0.345	364
n-Octane	12.89	14.10	1.21	0.340	557
n-Nonane	15.12	16.65	1.53	0.342	484
n-Decane	12.67	14.86	2.19	0.347	538
n-Dodecane	18.30	20.80	2.51	0.368	588
n-Tetradecane	17.41	19.48	2.07	0.407	667
n-Hexadecane	19.43	20.04	0.61	0.436	875
2,2,4-Trimethylpentane	11.19	12.67	1.48	0.485	381
Cyclohexane	14.70	17.43	2.74	0.413	846
1,2,3,4-Tetrahydronaphthalene	13.69	17.81	4.12	1.201	[a]

[a] Negative value is observed.

eters for 2,2,4-trimethylpentane are lower than *n*-octane; similar data for 1,2,3,4-tetrahydronaphthalene and cyclohexane are almost identical. However, the values of ΔH_S increase systematically from *n*-hexane to *n*-dodecane. This probably suggests, but does not prove, that the intermolecular forces between liquids and polymer molecule play an important role and that the diffusion and sorption mechanisms are not identical in the present Santoprene and *n*-alkane systems. A previous study by Billingham et al.[38] also supports this conjecture.

For all the penetrants the values of ΔH_S are positive, suggesting that the sorption is mainly dominated by the Henry's mode giving an endothermic contribution to the sorption process. An interesting question is whether the solvent molecules penetrate into the voids that already exist in the membrane material before solvent sorption or whether they create the pores in which they reside. To answer this question, the volumes of the membranes saturated with the solvents were measured and compared to the volume of the membrane without any solvent. If the solvent molecules simply fill the microvoids or free volume in the membrane, its volume then should not increase. However, in almost all cases, the volume of Santoprene is increased by solvent sorption due possibly to a contribution from the Henry's mode. It may, however, be noted that the volume increases are not greatly significant (i.e., $\frac{\partial V}{V}$ generally vary from 0.45 for *n*-pentane to about 1.13 for cyclohexane at 25°C).

Interaction Parameter and Molar Mass Between Crosslinks

As discussed earlier, the diffusion parameters in a solvent-elastomer system depend strongly on the morphological setup of the material, as manifested in the average molar mass $\bar{M}_C$ between crosslinks of the network, which is inversely related to the crosslink density. The most important characteristic of an elastomeric network is its degree of crosslinking to give elastic recoverability.[39] This aspect of network structure affects all of the elastomeric properties, including equilibrium properties such as modulus, ultimate strength, and degree of swelling.[40] Knowledge of it is thus of paramount importance with regard to both the molecular interpretation of rubberlike elasticity and the rational design of polymers having specified properties for a wide range of elastomeric applications. The magnitude of $\bar{M}_C$ significantly affects the physical and mechanical properties of the crosslinked polymers both in the presence and absence of solvent media and hence, its determination has a great practical value.

In the polymer literature, equilibrium swelling experiments have been widely used[41] to determine $\bar{M}_C$. Pioneering research by Flory et al.[42,43] laid the foundations for the analysis of equilibrium swelling data. Thus, for a perfect polymer network,

$$\bar{M}_C = \frac{-\rho_p V_S[\phi_p^{1/3} - \phi_p^{1/2}]}{\ln(1 - \phi_p) + \phi_p + \chi\phi_p^2} \tag{24}$$

where V_S is the molar volume of the solvent, ρ_p is the polymer density, ϕ_p is the volume fraction of the polymer in the swollen state, and χ has the conventional meaning from the Flory–Huggins interaction parameter between the solvent molecules and the polymer. Volume fraction of the polymer in the swollen state has been computed by using:[11]

$$\phi_P = \left[1 + \frac{\rho_p}{\rho_S}\left(\frac{M_a}{M_b}\right) - \frac{\rho_p}{\rho_S}\right]^{-1} \tag{25}$$

where M_b and M_a are, respectively, the mass of the polymer before and after swelling, ρ_S is solvent density and ρ_p is density of Santoprene.

The polymer–solvent interaction parameter, χ is calculated as,[44]

$$\chi = \beta + \frac{V_S}{RT}(\delta_S - \delta_p)^2 \tag{26}$$

where δ_S is solubility parameter of the solvent, β is a lattice constant whose value is generally taken to be 0.34 and RT is the usual energy term. In order to calculate χ as suggested above, it is important to have a prior knowledge of the solubility parameter δ_p of the polymer. The procedure of Gee[45] and Takahashi[46] has been used to compute δ_p of the polymer. A plot of swelling coefficient α (= $(M_a - M_b)/M_b\rho_s$) versus solubility parameter of the solvent was constructed. A maximum value in α was found at δ_S = 7.57 and this was taken to be the solubility parameter of the polymer.[47,48] Using this value for δ_p, we have calculated χ from eq. (26). The values of $\bar{M}_C$ have been calculated from eq. (24). These data are also included in Table X.

The values of $\bar{M}_C$ show a generally increasing trend with the length of *n*-alkanes. Because the nature of the crosslinked system is understood either in terms of $\bar{M}_C$ or in terms of its reciprocal value (i.e., crosslink density), it is evident that the crosslink density decreases with an increase in the size of the penetrant molecules. The values of $\bar{M}_C$ range from about 300 to 875 for *n*-hexane to *n*-hexadecane.

However, for n-pentane, $\bar{M}_C$ is small [i.e., 168 (not reported)] and for 1,2,3,4-tetrahydronaphthalene, we could not obtain reliable data. The $\bar{M}_C$ value of 2,2,4-trimethylpentane is smaller than n-octane. At any rate, the estimation of $\bar{M}_C$ from the Flory–Rehner theory has limited applications and hence these values should be regarded as only approximate. However, the data presented here serve for a qualitatively successful application of the Flory–Rehner theory.

CONCLUSIONS

The transport parameters of this study were found to decrease linearly with an increase in the size of the n-alkanes. The diffusivity values of 2,2,4-trimethylpentane at all temperatures were considerably lower than the corresponding values for a linear molecule of a similar size viz., n-octane. This is attributed to the rigidity of 2,2,4-trimethylpentane. Also 2,2,4-trimethylpentane exhibits a lower value of E_D than its corresponding isomer, n-octane which has a similar size. The change of the alkane size led to increasing resistance to the diffusion of the bigger solvent molecules penetrating through the polymer membrane.

At higher temperature, the increase in diffusion and relaxation rates of the polymer, accompanied by an increase in the polymer free volume, resulted in a higher equilibrium penetrant uptake. The observed overshoot effect with the present systems was attributed to polymer relaxational phenomenon. Transport kinetics have been studied in terms of the first-order and second-order kinetic equations. However, it is difficult to characterize the overall transport kinetics with a specific experimental parameter. It was shown that the changes in the transport kinetics during S–RS experiments are caused by the changes in the relative rates between the polymer chain relaxation and the penetrant diffusion during sorption. Though the diffusion coefficients have been estimated from the Fickian equation, these tend to exhibit concentration dependencies.

We are thankful to the Council of Scientific and Industrial Research [Grant No. 01(1239)/92/EMR-II] for a major financial support of this study.

REFERENCES

1. P. V. Kulkarni, S. B. Rajur, P. Antich, T. M. Aminabhavi, and M. I. Aralaguppi, *J. Macromol. Sci., Rev. Macromol. Chem. Phys.*, **C30,** 441 (1990).
2. T. M. Aminabhavi, R. S. Khinnavar, S. B. Harogoppad, U. S. Aithal, Q. T. Nguyen, and K. C. Hansen, *J. Macromol. Sci., Rev. Macromol. Chem. Phys.*, **C34,** 139 (1994).
3. S. B. Harogoppad and T. M. Aminabhavi, *Macromolecules,* **24,** 2598 (1991).
4. R. S. Khinnavar and T. M. Aminabhavi, *J. Appl. Polym. Sci.,* **42,** 2321 (1991).
5. T. M. Aminabhavi and H. T. S. Phayde, *Polymer,* in press.
6. T. M. Aminabhavi, R. S. Munnolli, W. M. Stahl, and S. V. Gangal, *J. Appl. Polym. Sci.,* **48,** 857 (1993).
7. R. S. Khinnavar and T. M. Aminabhavi, *Polymer,* **34,** 1006, (1993).
8. S. B. Harogoppad and T. M. Aminabhavi, *J. Appl. Polym. Sci.,* **46,** 725 (1992).
9. S. B. Harogoppad and T. M. Aminabhavi, *Polymer,* **32,** 870 (1991).
10. J. A. Riddick and W. B. Bunger, in *Techniques in Chemistry,* Vol. 2, *Organic Solvents Third Ed.,* Wiley-Interscience, John Wiley & Sons, New York, 1970.
11. U. S. Aithal, T. M. Aminabhavi, and P. E. Cassidy, *J. Membr. Sci.,* **50,** 225 (1990).
12. T. M. Aminabhavi and U. S. Aithal, *J. Appl. Polym. Sci.,* **41,** 2113 (1990).
13. R. S. Khinnavar and T. M. Aminabhavi, *Polymer,* **34,** 4280 (1993).
14. T. M. Aminabhavi and S. B. Harogoppad, *J. Chem. Educ.,* **68,** 343 (1991).
15. D. Kim, J. M. Caruthers, and N. A. Peppas, *Macromolecules,* **26,** 1841 (1993).
16. L. Y. Shieh and N. A. Peppas, *J. Appl. Polym. Sci.,* **42,** 1579 (1991).
17. G. W. R. Davidson and N. A. Peppas, *J. Control Rel.,* **3,** 243 (1986).
18. M. J. Smith and N. A. Peppas, *Polymer,* **26,** 569 (1985).
19. R. W. Korsmeyer and N. A. Peppas, *J. Control Rel.,* **1,** 89 (1984).
20. H. E. Johnson, S. J. Clarson, and S. Granick, *Polymer,* **34,** 1960 (1993).
21. A. Apicella, L. Nicolias, G. Astarita, and E. Drioli, *Polym. Eng. Sci.,* **18,** 18 (1981).
22. C. W. R. Davidson and N. A. Peppas, *J. Control. Rel.,* **3,** 243 (1986).
23. J. Crank, *The Mathematics of Diffusion,* 2nd Ed., Clarendon, Oxford, 1975.
24. P. E. M. Allen, D. J. Bennet, and D. R. G. Williams, *Eur. Polym. J.,* **28,** 347 (1992).
25. M. Salem, A. F. A. Asfour, D. DeKee, and B. Harrison, *J. Appl. Polym. Sci.,* **37,** 617 (1989).
26. W. R. Brown and G. S. Park, *J. Paint Technol.,* **42,** 16 (1970).
27. W. R. Brown, R. B. Jenkins, and G. S. Park, *J. Polym. Sci., Polym. Symp.,* **41,** 45 (1973).
28. A. Aitken and R. M. Barrer, *Trans. Faraday Soc.,* **51,** 116 (1955).
29. N. Vahdat, *J. Appl. Polym. Sci.,* **42,** 3165 (1991).
30. C. J. F. Bottcher, *Theory of Electric Polarisation,* Elsevier Publishing Company, Amsterdam, 1952.
31. M. R. Rao, *Curr. Sci.,* **8,** 510 (1939); *J. Chem. Phys.,* **9,** 682 (1941).

32. T. Feng, W. J. Macknight, and N. S. Schneider, *Polymer,* **32,** 1493 (1991).
33. H. Schott, *J. Macromol. Sci. Phys.,* **B31,** 1 (1992).
34. C. M. Ofner and H. Schott, *J. Pharm. Sci.,* **75,** 790 (1986).
35. C. M. Ofner and H. Schott, *J. Pharm. Sci.,* **76,** 715 (1987).
36. T. M. Aminabhavi, U. S. Aithal, and S. S. Shukla, *J. Macromol. Sci. Rev. Macromol. Chem. Phys.,* **C28**(3 & 4), 421 (1988).
37. M. J. Hayer and G. S. Park, *Trans Faraday Soc.,* **51,** 1134 (1955).
38. N. C. Billingham, P. D. Calvert, and A. Uzuner, *Eur. Polym. J.,* **25,** 839 (1989).
39. J. E. Mark, *J. Chem. Ed.,* **58,** 898 (1981).
40. T. L. Smith, *Polym. Eng. Sci.,* **17,** 129 (1977).
41. Z. Y. Ding, J. J. Aklonis, and R. Salovery, *J. Polym. Sci. Pt-B., Polym. Phys.,* **29,** 1035 (1991).
42. P. J. Flory, *Principles of Polymer Chemistry,* Cornell University Press, Ithaca, NY, 1953.
43. P. J. Flory and J. Rehner, Jr., *J. Chem. Phys.,* **11,** 521 (1943).
44. G. M. Bristow and W. F. Watson, *Trans. Faraday Soc.,* **54,** 1731 (1958).
45. G. Gee, *Trans. Faraday Soc.,* **38,** 418 (1942); *ibid* **40,** 468 (1944).
46. S. Takahashi, *J. Appl. Polym. Sci.,* **28,** 2847 (1983).
47. R. S. Neo, S. F. Chan, and J. Lee, *J. Membr. Sci.,* **9,** 273 (1981).
48. M. C. Gupta, V. P. Bansod, and I. D. Patil, *Polym. Commun.,* **28,** 204 (1987).

Received January 5, 1994
Accepted February 23, 1994